

Bcl-2 Family Proteins Contribute to Apoptotic Resistance in Lung Cancer Multicellular Spheroids

Tsung-Ming Yang^{1,2,4}, Dario Barbone^{2,4}, Dean A. Fennell³, and V. Courtney Broaddus^{2,3}

¹Division of Pulmonary and Critical Care Medicine, Chang Gung Memorial Hospital, Chiayi, Taiwan; ²Lung Biology Center, San Francisco General Hospital, San Francisco, California; ³Queen's University Belfast, Centre for Cancer Research and Cell Biology and Northern Ireland Cancer Centre, Belfast, Northern Ireland; and ⁴Comprehensive Cancer Center, University of California, San Francisco, California

Combinatorial therapies using the proteasome inhibitor, bortezomib, have been found to induce synergistic apoptosis in cancer cells grown as monolayers; however, three-dimensional spheroid culture may be a better model for the multicellular resistance found in solid tumors, such as lung cancer. We tested the combinatorial apoptotic strategy of using bortezomib together with TNF-related apoptosis-inducing ligand (TRAIL), both in monolayers and in spheroids of A549 lung cancer cells. Indeed, bortezomib plus TRAIL induced synergistic apoptosis in A549 cells grown as monolayers, but had little effect on A549 cells grown as three-dimensional multicellular spheroids. The acquired resistance of spheroids was not due to a limitation of diffusion, to survival pathways, such as NF- κ B or PI3K/Akt/mTOR, or to the up-regulation of FLIP_s (Fas-associated death domain-like IL-1 β -converting enzyme inhibitory protein, short). We then investigated a role for the Bcl-2 family of anti- and proapoptotic proteins. When cells formed spheroids, antiapoptotic Bcl-2 increased, whereas antiapoptotic Mcl-1 decreased. ABT-737, a small molecule that inhibits Bcl-2, but not Mcl-1, abolished the multicellular resistance of A549 spheroids to bortezomib plus TRAIL. In another lung cancer cell line, H1299, acquisition of multicellular resistance in spheroids was also accompanied by an increase in Bcl-2 and decrease in Mcl-1. In H1299 spheroids compared with those of A549, however, Mcl-1 remained higher, and Mcl-1 knockdown was more effective than ABT-737 in removing multicellular resistance. Our study suggests that the balance of Bcl-2 family proteins contributes to the acquired multicellular resistance of spheroids, and suggests a possible target for improving the response of lung cancer to bortezomib therapies.

Keywords: proteasome; TNF-related apoptosis-inducing ligand; mitochondria; bortezomib; ABT-737; Mcl-1

Combinatorial therapies with novel agents hold promise for inducing apoptosis in cancers (1). Agents that together are able to overcome the drug resistance acquired by cancer can achieve therapeutically desirable synergistic effects. Indeed, such approaches may also allow therapies to be targeted to tumor cells, thought to be primed for apoptosis by their dysregulated oncogenes and thus dependent on antiapoptotic defenses, while sparing normal tissues (2, 3). Ultimately, the hope is that individually subtoxic treatments can be combined to minimize overall toxicity while activating apoptosis selectively in the tumor cells.

One combinatorial approach effective *in vitro* has been the use of a proteasome inhibitor, bortezomib (Velcade), together

CLINICAL RELEVANCE

We show that lung cancer cells acquire multicellular apoptotic resistance as three-dimensional spheroids and show that this resistance can be bypassed by blocking members of the antiapoptotic Bcl-2 family. These proteins may be attractive targets to increase efficacy of treatments for lung cancer.

with other agents. Bortezomib has been shown to have myriad effects on the cell by its interruption of protein degradation. Its best known effect is the inactivation of the NF- κ B survival signaling pathway (4, 5), although more recent interest has centered on changes in expression of proteins directly involved in apoptosis such as the Bcl-2 family proteins (6–8). By these varied effects, bortezomib appears to disrupt the defenses of cancer cells and enhances their response to other apoptotic agents, particularly to the death receptor ligand, TNF-related apoptosis-inducing ligand (TRAIL) (9). TRAIL, via the extrinsic apoptotic pathway, engages its receptors, recruits caspase 8, which is then cleaved to its active form. Activated caspase 8 then cleaves the BH3-only molecule, Bid, which then interacts with mitochondrial anti- and proapoptotic molecules. The mechanism by which bortezomib enhances TRAIL-induced apoptosis may involve multiple molecular steps along these complex signaling pathways. In *in vitro* studies, bortezomib plus TRAIL has been highly effective in inducing a synergistic apoptosis in lung cancer cell lines (10, 11) and other cancer cell lines (12–14), suggesting that this approach would be useful in the clinic. Nonetheless, although bortezomib has been effective in hematologic cancers, such as multiple myeloma (15, 16), it has been generally ineffective in solid tumors, such as lung cancer (17, 18). The cause of this clinical resistance is currently unknown.

Resistance to apoptosis can be modeled *in vitro* by the study of cancer cells in three-dimensional (3D) aggregates called spheroids (19). Indeed, when compared with their two-dimensional (2D) counterparts, 3D multicellular spheroids may mimic features of cancer that can give therapeutic insights (19, 20). In 3D spheroids of mesothelioma tumor cells, we previously identified an acquired resistance to combinatorial therapies that was due, at least in part, to the mammalian target of rapamycin (mTOR) pathway, which demonstrated an antiapoptotic effect in spheroids that was not evident in monolayers (21). We then confirmed that the mTOR pathway also exerted a survival function in tumor fragments grown from human mesothelioma (22); clinical trials will confirm whether inhibition of the pathway offers benefit in patients with mesothelioma. By such studies, it is hoped that 3D models will elucidate mechanisms of apoptotic resistance that may provide clues to the therapeutic resistance seen clinically. We considered that studies in 3D spheroids would help uncover mechanisms of apoptotic resistance to bortezomib in lung cancer. Indeed, the effect of

(Received in original form August 19, 2008 and in final form November 14, 2008)

This work was supported by National Institutes of Health grant R01 CA95671 (V.C.B.) and the Chang Gung Memorial Hospital of Taiwan (T.M.Y.).

Correspondence and requests for reprints should be addressed to V. Courtney Broaddus, M.D., 1001 Potrero Ave., Bldg. 1, Rm 150, San Francisco, CA 94110. E-mail: cbroaddus@medsfgh.ucsf.edu

This article has an online supplement, which is accessible from this issue's table of contents at www.atsjournals.org

Am J Respir Cell Mol Biol Vol 41, pp 14–23, 2009

Originally Published in Press as DOI: 10.1165/rcmb.2008-03200C on December 18, 2008

Internet address: www.atsjournals.org

proteasome inhibition on lung cancer cells in a 3D setting has not yet been explored.

In this study, focusing on the lung cancer lines, A549 and H1299, we have confirmed the effectiveness of the combinatorial apoptotic strategy of using bortezomib plus TRAIL when the cells are grown in monolayers, and have shown for the first time that a high-level resistance is acquired when the cells form 3D spheroids. In investigating the cause of this acquired resistance, we found no evidence that the activity of bortezomib alone or of TRAIL alone was impaired in the spheroids, whereas the combined effects were clearly inhibited. Blockade of antiapoptotic Bcl-2 family proteins in the spheroids restored apoptosis, suggesting that the resistance to this combinatorial therapy was maintained by the balance of the pro- and antiapoptotic molecules at the mitochondria, the site of integration of apoptotic signals. Similar strategies to counteract antiapoptotic defenses may restore effectiveness of bortezomib therapies in lung cancer and other solid tumors.

MATERIALS AND METHODS

Cell Cultures and Reagents

The human non-small cell lung cancer (NSCLC) cell lines, A549 and H1299, were obtained from the American Type Culture Collection, and cultured in Dulbecco's modified Eagles medium (DMEM) supplemented with 10% FBS and 100 IU/ml penicillin/streptomycin in a 37°C humidified incubator with 5% CO₂. A549 cells transduced with an NF-κB luciferase reporter (A549/NF-κB-luc; a generous gift from Dr. James Frank, University of California, San Francisco) were cultured in DMEM supplemented with 10% FBS, 100 IU/ml penicillin/streptomycin, and 100 μg/ml hygromycin B (ALX-380-059-UM01; Alexis Biochemicals, San Diego, CA). Recombinant human TRAIL (no. 375-TEC) was from R&D Systems (Minneapolis, MN). Bortezomib (Velcade) was from Millennium Pharmaceuticals (Cambridge MA). BAY 11-7082, an inhibitor of NF-κB activity, was obtained from Alexis Biochemicals. Rapamycin, an mTOR inhibitor, was purchased from Sigma-Aldrich (St. Louis, MO), and the PI3K inhibitor, PI-103, a novel inhibitor of the PI3K/Akt/mTOR pathway, was a gift of Dr. Kevan Shokat (University of California, San Francisco). ABT-737, a small molecule inhibitor of the antiapoptotic proteins, Bcl-2, Bcl-xL, and Bcl-w, and the enantiomer, A-793844.0, a negative control for ABT, was kindly provided by Abbott.

Generation of Spheroids

Multicellular spheroids were generated in nonadsorbent, round-bottomed, 96-well plates. The plates were coated with a 1:24 dilution of polyHEMA (120 mg/ml) (Sigma-Aldrich) in 95% ethanol and dried at 37°C for 48 hours. Before use, plates were sterilized by ultraviolet light for 30 minutes. To generate multicellular spheroids, 10,000 cells were added into each well of polyHEMA-coated 96-well plates. The plates were briefly spun for 5 minutes at 800 rpm and then placed in a 37°C humidified incubator with 5% CO₂ until spheroids formed—24 hours for H1299 cells or 48 hours for A549 cells. To generate monolayers, 50,000 cells were added into each well of 12-well plates. Before experiments, five spheroids were transferred to a polyHEMA-coated 24-well plate to match the numbers of cells plated in the monolayers (50,000 cells/well). The spheroids and monolayers were treated with apoptotic agents with or without inhibitors (with the appropriate DMSO vehicle control) for 24 hours.

Microspheroids with an average of 250 cells each were generated using nonadhesive hydrogels cast by micromolds, as previously described (23). In brief, 3% agarose gels (Ultrapure agarose; Invitrogen, Carlsbad, CA) were cast by using micromolds, which produced recesses on the gel surface. The gels were then equilibrated overnight with complete culture medium. Trypsinized cells were resuspended to the appropriate cell density and then pipetted onto the gels. Over 24 hours (H1299) or 48 hours (A549), cells within the recesses spontaneously formed into aggregates, were recovered from the gels by centrifugation, and were then moved to 24-well plates for experiments.

Immunoblotting

After treatment, monolayers and spheroids were lysed in boiling lysis buffer (2.5% SDS, 250 mM Tris-HCl, pH 7.4). The concentration of total protein was evaluated with a colorimetric assay (DC protein assay; Bio-Rad, Hercules, CA). Total cell lysates (35–50 μg) were loaded in reducing conditions (0.2 M Tris, pH 6.8, 5% SDS, 3% glycerol, 0.01% bromophenol blue, and 200 mM DTT). After separation in SDS-PAGE (5–15% acrylamide) and transfer to polyvinylidene fluoride (Immobilon; Millipore, Billerica, MA), membranes were blocked with a protein-free tris-buffered saline blocking buffer (Pierce, Rockford, IL), and gently agitated with antibodies diluted in 5% nonfat dry milk or 5% BSA, as appropriate, at 4°C overnight. Secondary antibodies were from Amersham (Piscataway, NJ). The signal was detected by the enhanced SuperSignal West Pico Chemiluminescent Substrate (Pierce). The antibodies against Bcl-2 (no. 2870), Bcl-xL (no. 2764), Bid (no. 2006), and Bim (no. 2933) were from Cell Signaling Technology (Beverly, MA). The Mcl-1 (sc-819) and Fas-associated death domain-like IL-1β-converting enzyme inhibitory protein (long/short) (FLIP_{L/S}; sc-5276) antibodies were from Santa Cruz Biotechnology (Santa Cruz, CA). The antibody to Noxa (OP180) was from Calbiochem (La Jolla, CA). The α-tubulin (no. T-6074) and β-actin (A5441) antibodies were from Sigma-Aldrich.

Proteasome Activity Assay

Proteasome activity in A549 spheroids and monolayers was measured by using a commercial 20S proteasome activity assay kit (APT280; Chemicon, Temecula, CA). In brief, spheroids and monolayers were lysed with proteasome activity buffer (50 mM Hepes pH 7.5, 5 mM EDTA, 150 mM NaCl, and 1% Triton X-100). The lysates were incubated with the fluorogenic substrate, LLVY-AMC (a fluorophore 7-amino-4-methylcoumarin [AMC] bound with LLVY peptide) at 37°C for 2 hours. LLVY is a substrate recognized and cleaved by the 20S proteasome. After LLVY chymotryptic cleavage by the 20S proteasome, AMC is released and emits fluorescence that can be read by using a 380-nm excitation and a 460-nm emission filter in a fluorometer.

Immunofluorescent Staining

Immunofluorescent staining for cleaved caspase 3 was performed to detect the location of apoptotic cells in the spheroids. After treatment with bortezomib plus TRAIL for 24 hours, the spheroids were collected, fixed in 10% buffered formalin phosphate, and then embedded in paraffin. Sections (8 μm) were cut and mounted on glass slides, deparaffinized, and rehydrated. The slides were then boiled in sodium citrate solution (pH 6.0) with 0.1% Tween 20 in a pressure cooker for 5 minutes for antigen retrieval. After cooling for 20 minutes at room temperature, sections were blocked with 5% BSA for 30 minutes. The slides were incubated with rabbit polyclonal antibody to cleaved caspase 3 (1:100, AB3623; Chemicon, Temecula, CA) overnight at 4°C. The slides were then washed, incubated with a goat anti-rabbit IgG conjugated with Alexa Fluor 546 (1:100, A11010; Molecular Probes, Invitrogen) for 1 hour at room temperature, and mounted with DAPI (4',6'-diamidino-2-phenylindole)-containing antifade reagent (S36939; Invitrogen). A no-primary-antibody control was used as a negative control, and showed no staining; thymus tissue was stained as a positive control, and showed characteristic staining for apoptotic cells.

NF-κB Activity Assay

NF-κB activity in monolayers and spheroids was measured in an A549-stable reporter line in which the cells express the luciferase gene under an NF-κB promoter (A549/NF-κB-luc) (24), using a commercial luciferase assay kit (556866, BD Monolight; BD Science, San Jose, CA). In brief, equal numbers of cells in either monolayers or spheroids were lysed with provided cell lysis buffer. The appropriate volume of each lysate was added into wells of 96-well plates. Luciferase substrates were added to the lysates, which then emitted light that was read using a luminometer, and expressed as relative NF-κB activity.

RNA Interference

A549 or H1299 cells ($2-4 \times 10^6$) were pelleted and resuspended in 100 μl of nucleofection buffer solution T (A549) or solution C (H1299) (Amaxa Biosystems, Cologne, Germany) with 1.5 μg of the appropri-

ate small interfering RNA (siRNA) duplex (Ambion, Austin, TX). This suspension was transferred to a sterile cuvette and nucleofected using program X-001 (A549) or X-005 (H1299) on a Nucleofector II device (Amaxa Biosystems). After 30 minutes of recovery in complete DMEM medium, the cells were plated and allowed to grow for 24 hours. Cells were then trypsinized, counted, and plated as monolayers and spheroids for 24 hours (H1299) or 48 hours (A549), and exposed to apoptotic stimuli. The siRNA duplex sequences were: FLIP (total), GCA GUC UGU UCA AGG AGC AdTdT; FLIP_s, CAU GGA ACU GCC UCU ACU UdTdT, and for Mcl-1: CCA GUA UAC UUC UUA GAA AdTdT. The control sequence was random: ACG UGA CAC GUU CGG AGA AdTdT. Nucleofection of a green fluorescent protein (GFP)-expressing plasmid confirmed transfection efficiency of more than 90% of cells at 24 hours.

Hoechst Staining

Monolayers and spheroids were exposed to trypsin for 15 minutes—the time necessary to disaggregate the spheroids to single cells—washed with ice-cold PBS, and then fixed with 2.5% glutaraldehyde (Sigma-Aldrich). The cells were then stained with a fluorescent nuclear stain, Hoechst 33342 (8 $\mu\text{g/ml}$; Molecular Probes, Invitrogen), and placed on slides. For each condition, at least 300 cells were counted in triplicate by investigators blinded to the experimental conditions. Cells with distinctive signs of nuclear condensation were considered apoptotic. Apoptosis was confirmed by flow cytometry using annexin V staining; however, as we observed previously (21), annexin staining of cells from spheroids was somewhat inconsistent, perhaps because the surface properties of cells were altered after spheroid formation. Therefore, as before, we relied on nuclear morphology for quantification of apoptotic cells.

Statistical Analysis

Data are expressed as mean (\pm SD) of at least three different experiments. Statistical significance was evaluated by one-way ANOVA, and Tukey's test was performed to detect where the differences lay (GraphPad Prism version 4.0; GraphPad Software, Inc., La Jolla, CA). A *P* value less than 0.05 was considered significant.

RESULTS

A549 Cells Formed Multicellular Spheroids within 48 Hours and Acquired Resistance to Bortezomib Plus TRAIL

After being seeded in polyHEMA-coated 96-well plates, A549 formed into multicellular spheroids within 48 hours (Figure 1A). At 10,000 cells per spheroid—a number found ideal in previous studies (21)—spheroids assumed a discoid shape with a diameter of 750 to 1,000 μm and an average thickness of 100 μm . The discoid shape was seen as an advantage, as it minimizes the diffusion distances to cells within the spheroids. To confirm that acquired resistance was not dependent on a particular size or shape, microspheroids of approximately 250 to 300 cells per spheroid were generated by means of micromolded nonadhesive hydrogels (23) and used in some of the apoptosis studies. These microspheroids were spherical in shape, with a diameter of 75 to 100 μm . In general, the diffusion distance was 50 μm in the multicellular spheroids, and less than 50 μm in the microspheroids—distances considered to be adequate for diffusion of oxygen and nutrients in tumors (25).

In monolayers, we tested bortezomib in combination with a variety of proapoptotic agents, including chemotherapeutic agents, histone deacetylases, and TRAIL. Of these combinations, the most effective combination for synergistic apoptosis in monolayers was bortezomib plus TRAIL, found by others to be effective in NSCLC cells (10). Thus, we applied this combination of apoptotic agents to A549 cells grown as monolayers and as spheroids. In monolayers, A549 cells showed a striking amplification of apoptosis in which the effect of the combination was significantly greater than the sum of the effects of each agent individually (Figure 1B). In spheroids, however, the lung

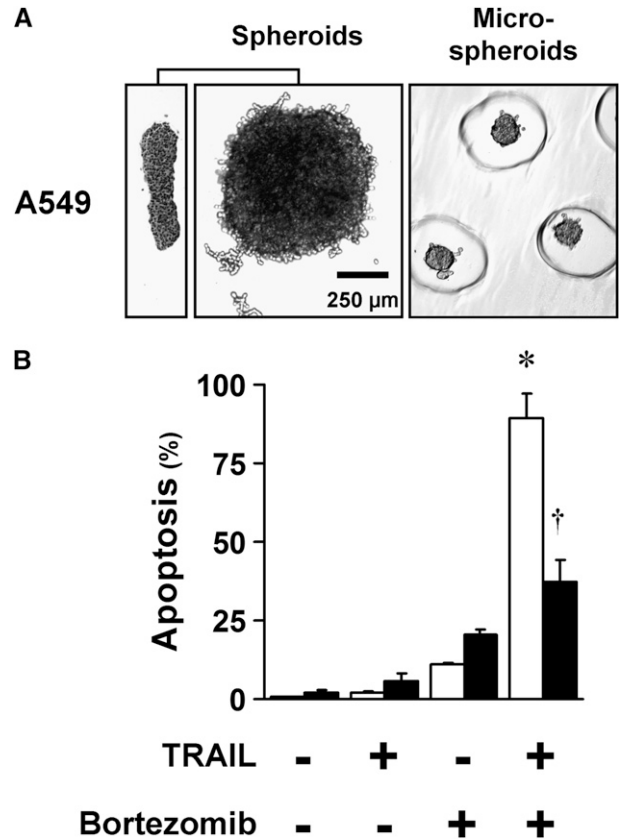


Figure 1. A549 cells formed multicellular spheroids within 48 hours and acquired resistance to bortezomib plus TNF-related apoptosis-inducing ligand (TRAIL). (A) Spheroids and microspheroids formed from A549 cells have short diffusion distances. Spheroids generated with 10,000 cells each show consistent discoid shape and size, shown from a side view (left panel) and from above (center panel), with a width of 750–1,000 μm and a thickness of 100 μm . Microspheroids generated from 250 cells each are spherical, with a diameter of 75–100 μm . The microspheroids are shown in the recesses of the gel used to form them (representative images shown). (B) A549 cells in monolayer undergo synergistic apoptosis to the combination of bortezomib plus TRAIL, whereas spheroids exhibit resistance. A549 monolayers (open bars) and spheroids (solid bars) were exposed to the proteasome inhibitor, bortezomib (100 nM), plus TRAIL (1 ng/ml) for 24 hours, and then examined for apoptosis after Hoechst 33342 nuclear staining. Neither monolayers nor spheroids responded significantly to TRAIL alone or to bortezomib alone. In cells grown as monolayers, the apoptotic response to the combination of bortezomib plus TRAIL was synergistic, because the response to the combination was statistically greater than the sum of the responses to the individual agents. Compared with monolayers, the spheroids were resistant (*different from the sum of the responses to TRAIL alone and to bortezomib alone; †different from monolayer; mean \pm SD; *n* = 3; *P* < 0.01).

cancer cells showed a significant resistance to bortezomib plus TRAIL (Figure 1B).

Multicellular Resistance to Bortezomib Plus TRAIL Is Not Due to Limitation of Diffusion

It was possible that the apoptotic agents had inadequate diffusion or poor activity in spheroids. To test the diffusion and the activity of bortezomib, we assayed proteasome activity of monolayers and spheroids before and after exposure to bortezomib. At baseline conditions, proteasome activity was lower in spheroids than in monolayers; however, exposure to

bortezomib for 4 hours inhibited proteasome activity equally in both spheroids and monolayers (Figure 2A). To test whether the diffusion or activity of TRAIL was limited in spheroids, we examined TRAIL-induced Bid cleavage in monolayers and spheroids. Bid cleavage, as judged by the decrease in full-length Bid, was similar in monolayers and spheroids after TRAIL exposure, suggesting that the diffusion of TRAIL into spheroids was not limited (Figure 2B). Of note, after bortezomib plus TRAIL, Bid cleavage was enhanced in monolayers, but not in spheroids, consistent with a feedback activation of caspase 8 and Bid cleavage with apoptosis (2). As another test for possible limitation of diffusion into spheroids, we assessed the response of microspheroids, consisting of roughly 250 cells per spheroid. Despite their smaller size, these microspheroids demonstrated apoptotic resistance similar to that of multicellular spheroids (Figure 2C). Finally, to evaluate possible diffusion effects on apoptosis, we identified the location of apoptotic cells in the spheroids by staining for cleaved caspase 3 in spheroids exposed to bortezomib plus TRAIL for 24 hours. We found apoptotic cells evenly distributed throughout the spheroids, not in any one particular region (Figure 2D), suggesting that resistance was a general phenomenon, and not determined by limited diffusion or regional differences in the spheroids. In summation, these findings indicate that a limitation of diffusion does not explain the acquired multicellular resistance of A549 spheroids.

Multicellular Resistance to Bortezomib Plus TRAIL Is Not Due to the NF-κB Pathway

Inactivation of the NF-κB pathway has been thought to be a major mechanism for bortezomib-induced apoptosis (4). To evaluate the contribution of NF-κB to the multicellular resistance of NSCLC spheroids, we measured the NF-κB activity in A549 cells containing a stable NF-κB luciferase activity reporter. First, we determined whether TRAIL induced NF-κB activity in A549 cells. Although NF-κB was activated by TNF-α, a potent NF-κB inducer, there was no response to TRAIL at 1 ng/ml or at 10 ng/ml, a concentration 10-fold higher than that used to induce apoptosis in this study (Figure 3A). The inhibition by the NF-κB inhibitor, BAY 11-7082, confirmed that the luciferase signal stimulated by TNF-α was due to NF-κB activity. We next tested whether NF-κB activity was different in the spheroids compared with monolayers (Figure 3B). Monolayers and spheroids displayed no significant difference in NF-κB activity at baseline or after stimulation with TNF-α (Figure 3B). In addition, NF-κB activity was equally inhibited by bortezomib in both monolayers and spheroids. Given the comparable activity and inhibition of NF-κB in monolayers and spheroids, it is unlikely that the NF-κB pathway accounts for the resistance of the spheroids to bortezomib plus TRAIL.

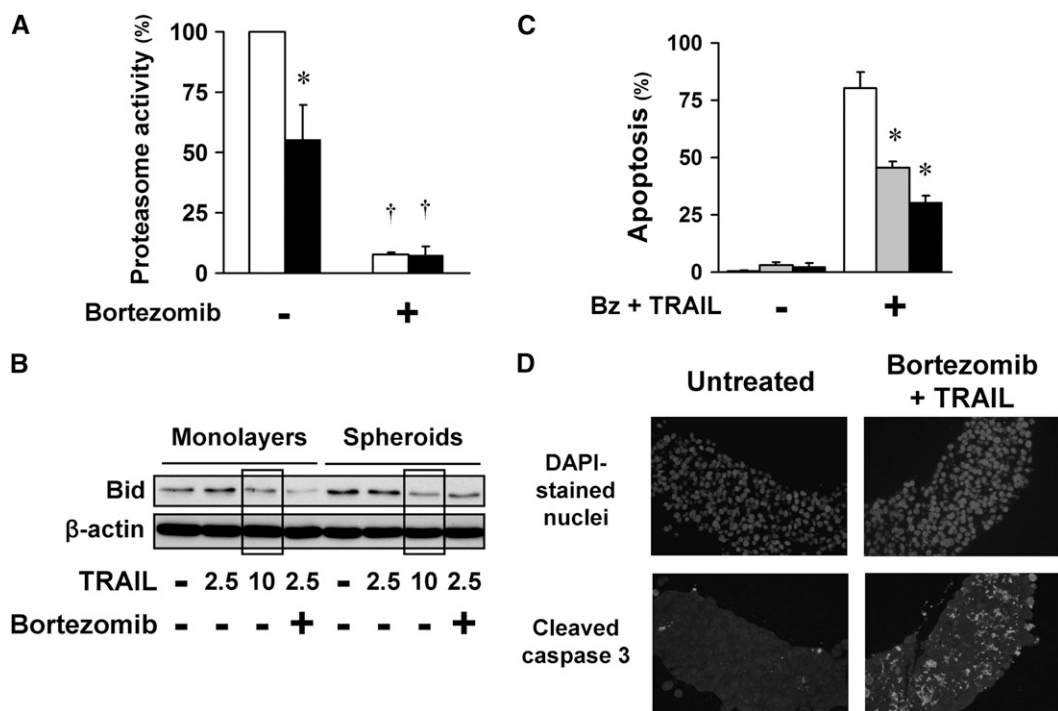


Figure 2. Apoptotic resistance of spheroids to bortezomib plus TRAIL is not due to the limited diffusion of reagents into the spheroids. (A) Bortezomib inhibits the proteasome activity equally in A549 monolayers (open bars) and spheroids (solid bars). Under baseline conditions, proteasome activity was lower in A549 cells in spheroids than in monolayers. After exposure to bortezomib (100 nM) for 4 hours, proteasome activity in both monolayer and spheroid was equally inhibited (*different from baseline; mean ± SD; n = 3; P < 0.01). (B) TRAIL induced similar Bid cleavage in monolayers and spheroids. A549 monolayers and spheroids were exposed to TRAIL (2.5, 5, or 10 ng/ml) with or without bortezomib (100 nM) for 16 hours. TRAIL-induced Bid

cleavage was measured by immunoblot as a decrease in full-length Bid. TRAIL 2.5 and 10 ng/ml induced similar Bid cleavage in A549 monolayers and spheroids (see boxed areas). After combination therapy, Bid cleavage is enhanced in monolayers compared with spheroids, consistent with an enhanced Bid cleavage seen after apoptosis and widespread activation of caspases (2). (C) Microspheroids demonstrate apoptotic resistance similar to that of spheroids. A549 cells grown as monolayers (open bars), microspheroids (shaded bars), and spheroids (solid bars) were exposed to 100 nM bortezomib (Bz) plus 1 ng/ml TRAIL for 24 hours, and then studied for apoptosis after Hoechst 33342 nuclear staining. Despite their difference in size and shape, and the shorter diffusion distance in the microspheroids, microspheroids and spheroids showed similar apoptotic resistance to bortezomib and TRAIL (*different from monolayer; mean ± SD; n = 3; P < 0.01). (D) Apoptotic cells are distributed evenly throughout the spheroids. A549 multicellular spheroids were treated with bortezomib (100 nM) plus TRAIL (1 ng/ml) for 24 hours, and then prepared for immunohistochemistry. Nuclei of all cells are indicated by DAPI staining; apoptotic cells are those with cleaved caspase 3. After exposure to bortezomib plus TRAIL, apoptotic cells are located throughout the spheroids, not in any one particular region (negative control with no primary antibody showed no staining; positive control, thymus, showed characteristic staining for apoptotic cells).

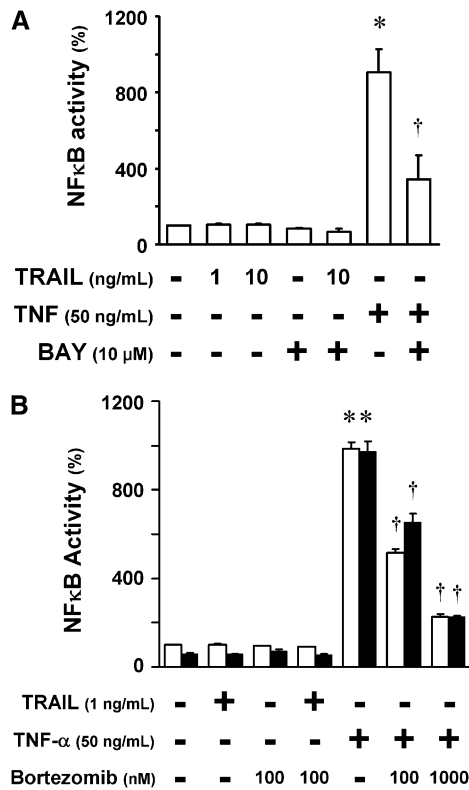


Figure 3. Apoptotic resistance of spheroids to bortezomib plus TRAIL is not likely due to the NF- κ B pathway. (A) TRAIL fails to activate the NF- κ B pathway in A549 cells. A549/NF- κ B-luc monolayers were pretreated with nothing or with the NF- κ B inhibitor, BAY 11-7082 (10 μ M), for 1 hour, and then exposed to TRAIL (1 or 10 ng/ml) or TNF- α (50 ng/ml) for 5 hours. TNF- α induced a strong luciferase signal; the expected inhibition by BAY confirmed that the luciferase activity represented NF- κ B signaling. TRAIL did not induce NF- κ B signaling. (B) NF- κ B is activated by TNF in monolayers (*open bars*) and spheroids (*solid bars*) equally, and is inhibited equally by bortezomib. A549/NF- κ B-luc monolayers and spheroids were pretreated with nothing or with bortezomib (100 nM or 1,000 nM) for 1 hour, and then exposed to TRAIL (1 ng/ml) or TNF- α (50 ng/ml) for 5 hours. NF- κ B was activated by TNF- α in both monolayers and spheroids, and was equally inhibited by bortezomib. NF- κ B was not activated by TRAIL in either monolayers or spheroids (*different from baseline; †different from TNF- α stimulation; mean \pm SD; $n = 3$; $P < 0.01$).

Inhibitors of PI3K/Akt/mTOR Do Not Reduce the Apoptotic Resistance of Multicellular Spheroids

Our previous studies in mesothelioma showed that mTOR contributes to the apoptotic resistance in multicellular spheroids generated from cell lines, and in tumor fragment spheroids generated from actual tumor (21, 22). Hence, we evaluated whether mTOR also contributes to the multicellular resistance of A549 spheroids by using rapamycin, a TOR complex 1 inhibitor, and PI-103, an inhibitor of PI3K and TOR complex 1 and -2. The inhibitors were effective in blocking the pathways, as expected (Figure 4A). Of note, baseline activity of the Akt/mTOR pathway appeared to be lower in spheroids than in monolayers, as previously observed in mesothelioma spheroids (21) (Figure 4A). The inhibitors had no effect alone, and did not reduce multicellular resistance of the spheroids (Figure 4B). This finding suggests that the Akt/mTOR pathway does not contribute to the multicellular resistance of NSCLC spheroids in this setting.

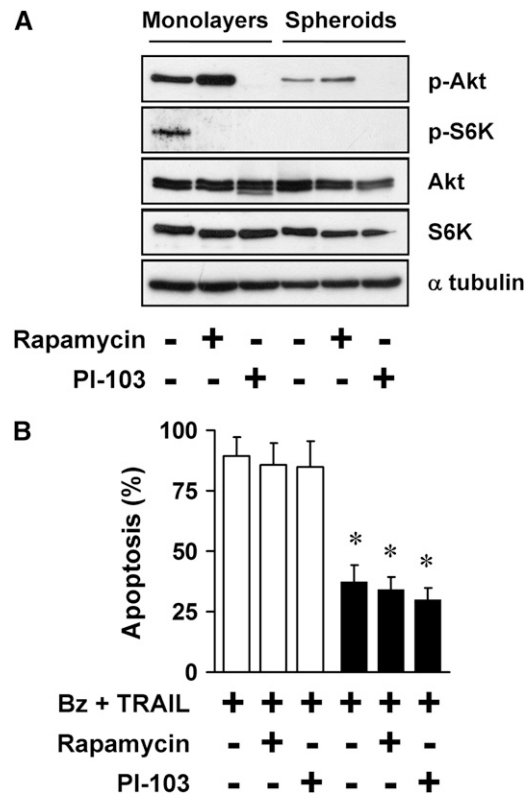


Figure 4. Apoptotic resistance in spheroids is not due to the PI3K/Akt/mTOR pathway. (A) The PI3K/Akt/mTOR pathway is inhibited by rapamycin and PI-103 in A549 monolayers and spheroids. A549 monolayers and spheroids were exposed to nothing, rapamycin (25 nM), or PI-103 (1 μ M) for 4 hours, and then studied by immunoblot for expression of p-Akt (Ser473) and p-S6K (Thr389). Rapamycin inhibited mTOR activity, as shown by a decrease in the mTOR target, p-S6K, and PI-103 inhibited both PI3K and mTOR, as shown by a decrease in p-Akt and p-S6K. (B) PI3K/Akt/mTOR inhibitors do not reduce apoptotic resistance of spheroids to bortezomib plus TRAIL. A549 monolayers (*open bars*) and spheroids (*solid bars*) were treated with 100 nM bortezomib (Bz) plus 1 ng/ml TRAIL with either no inhibitor, 25 nM rapamycin, or 1 μ M PI-103 for 24 hours. The inhibitors did not reduce the apoptotic resistance of spheroids to bortezomib plus TRAIL (*different from monolayer; mean \pm SD; $n = 3$; $P < 0.001$).

FLIP_S Is Up-Regulated in Multicellular Spheroids, but Does Not Mediate Multicellular Resistance

FLIP can inhibit TRAIL-induced signaling by interfering with recruitment and activation of caspase 8 and cleavage of Bid, and perhaps by interfering directly with activation of Bax (26). Therefore, we examined FLIP expression and found that FLIP_S was up-regulated in spheroids compared with monolayers, and this difference persisted after bortezomib (as shown in Figure E1A in the online supplement). To evaluate the role of FLIP in apoptotic resistance, we used siRNA techniques to deplete FLIP. Depletion of total FLIP induced more than 40% apoptosis in A549 cells, a toxicity that has been described after depletion of FLIP (27, 28). On the other hand, selective depletion of FLIP_S was not toxic to the cells and, because FLIP_S was the major form of FLIP up-regulated in spheroids, we chose to deplete this form in spheroids. Depletion of FLIP_S did not reduce the multicellular resistance (Figure E1B), suggesting that acquisition of multicellular resistance by spheroids was not dependent on the up-regulation of FLIP_S.

Blockade of Antiapoptotic Bcl-2 Proteins Removes Multicellular Resistance of A549 Spheroids

Because of the central role of the mitochondria in apoptosis, we evaluated the expression levels of pro-/antiapoptotic Bcl-2-family proteins. In spheroids compared with monolayers, there was up-regulation of Bcl-2 and a down-regulation of Mcl-1 and, to a lesser extent, Bcl-xL, a differential expression that was maintained after bortezomib (Figure 5A). After exposure to bortezomib plus TRAIL for 4 hours, the proapoptotic BH3-only molecule, Noxa, was up-regulated in monolayers, but not in spheroids, whereas another proapoptotic BH3-only molecule, Bim_{EL}, was up-regulated in both monolayers and spheroids. Because the Bcl-2 antiapoptotic proteins block apoptosis to a wide variety of apoptotic stimuli, we evaluated the role of Bcl-2 in the multicellular resistance of A549 spheroids by using ABT-737, a small-molecule inhibitor of antiapoptotic Bcl-2, Bcl-xL, and Bcl-w (29). Addition of 10 μM ABT-737 abolished the multicellular resistance of spheroids when treated with bortezomib plus TRAIL (Figure 5B). The enantiomer, a similar chemical compound designed to control for the specific binding of ABT-737, had no effect. To our surprise, ABT-737 by itself induced apoptosis in A549 spheroids without affecting monolayers, showing an acquired dependence of spheroids on the Bcl-2, Bcl-xL, and Bcl-w proteins for survival. We conclude that the antiapoptotic repertoire was altered in spheroids, leading to a greater dependence on antiapoptotic Bcl-2 proteins, a dependence revealed by the response to ABT-737.

H1299 Multicellular Spheroids Acquired Resistance to Bortezomib Plus TRAIL and Showed an Altered Balance of Bcl-2 Family Proteins Similar to A549 Spheroids

To determine whether the altered balance of Bcl-2 family proteins and its contribution to the multicellular resistance are unique to A549 cells, we investigated another NSCLC cell line, H1299. When seeded in polyHEMA-coated 96-well plates, H1299 formed multicellular spheroids within 24 hours (Figure 6A). H1299 spheroids and microspheroids acquired a multicellular apoptotic resistance to bortezomib plus TRAIL, a resistance even greater than that seen with A549 cells (Figures 6B and 6C). The expression of Bcl-2 family members changed in a similar fashion in H1299 as in A549 cells: with spheroid formation, the expression of Bcl-2 increased, whereas that of Mcl-1 decreased; after bortezomib plus TRAIL, Noxa increased in monolayers, but not in spheroids, whereas Bim_{EL} was maintained in both (Figure 6D).

Blockade of Antiapoptotic Mcl-1 Is More Effective Than Blockade of Bcl-2 at Removing Multicellular Resistance in H1299 Spheroids

In contrast to A549 spheroids, ABT-737 alone did not abolish the multicellular resistance of H1299 spheroids to bortezomib plus TRAIL (Figure 7A). Because Mcl-1 may account for resistance to ABT-737 (30), we compared the level of Mcl-1 in the two cell lines; despite a decrease of Mcl-1 in both cell lines as they formed spheroids, the level of Mcl-1 in H1299 spheroids exceeded that in A549 spheroids (Figure 7B). We then ablated Mcl-1 in H1299 by siRNA (Figure 7C). Ablation of Mcl-1 had no effect by itself, but largely eliminated the multicellular resistance of H1299 spheroids to bortezomib plus TRAIL (Figure 7D). When ABT was added to cells with ablated Mcl-1, the multicellular resistance of H1299 to bortezomib plus TRAIL was completely abolished (Figure 7D). Thus, the antiapoptotic Bcl-2 family proteins contribute to the multicellular resistance of H1299 spheroids, although the relative roles of Bcl-2 and Mcl-1 differ in the two cell lines.

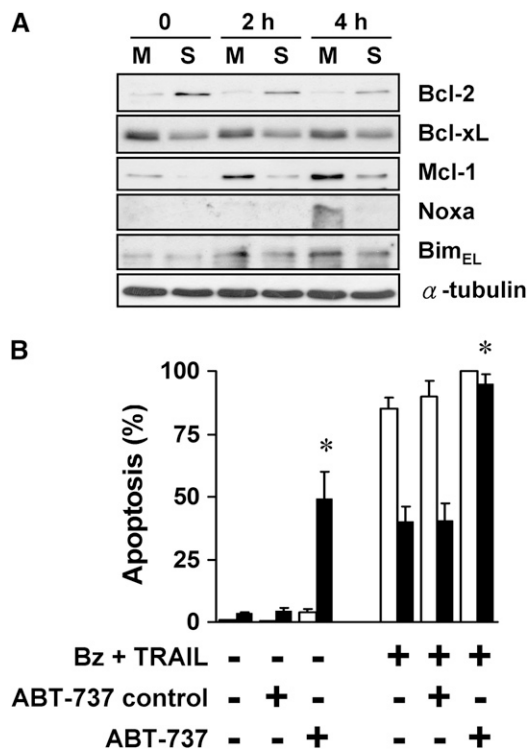


Figure 5. Balance of anti- and proapoptotic proteins and response to treatment is altered in spheroids, contributing to apoptotic resistance. (A) Expression of Bcl-2 increases and Mcl-1 decreases when A549 cells form spheroids. A panel of anti- and proapoptotic Bcl-2 family proteins were screened by immunoblot in A549 monolayers (M) and spheroids (S), before and after treatment with 100 nM bortezomib plus 1 ng/ml TRAIL for 2 and 4 hours. Bcl-2 was up-regulated after A549 spheroids formed spheroids, whereas Bcl-xL and Mcl-1 were down-regulated. At 4 hours after treatment, there was a significant up-regulation of Noxa in monolayers, but not in spheroids. (B) ABT-737, a BH3 mimetic that blocks Bcl-2, Bcl-xL, and Bcl-w, induces apoptosis in spheroids and eliminates apoptotic resistance. At baseline, the Bcl-2 family inhibitor, ABT-737, alone (10 μM) induced apoptosis in A549 spheroids without any effect on monolayers. After exposure to bortezomib plus TRAIL, 10 μM ABT-737 induced a significant increase in apoptosis of spheroids, so that the response to treatment was equal in monolayers (open bars) and spheroids (solid bars). The negative control enantiomer of ABT had no effect (*different from negative control for ABT; mean ± SD; n = 3; P < 0.01).

DISCUSSION

The ability of cancer cells to evade apoptosis is a vital property (31) that confers resistance to chemotherapeutic agents (32, 33). Understanding apoptotic resistance may inform strategies to restore apoptotic sensitivity in cancer cells and ultimately to improve cancer therapy (3). Multicellular spheroids have emerged as a promising tool in cancer research because of their acquired resistance to apoptosis that may provide insights into apoptotic resistance acquired *in vivo* (20, 34). In this study, we have identified, for the first time, that 3D multicellular spheroids acquire a resistance to combinatorial therapy with bortezomib, and show that it can be bypassed by blockade of the Bcl-2 family proteins. To our knowledge, this study represents the first to describe multicellular apoptotic resistance to a bortezomib-containing regimen. We believe that this investigation is significant because it offers insights that may be relevant to understanding the resistance in the clinical setting.

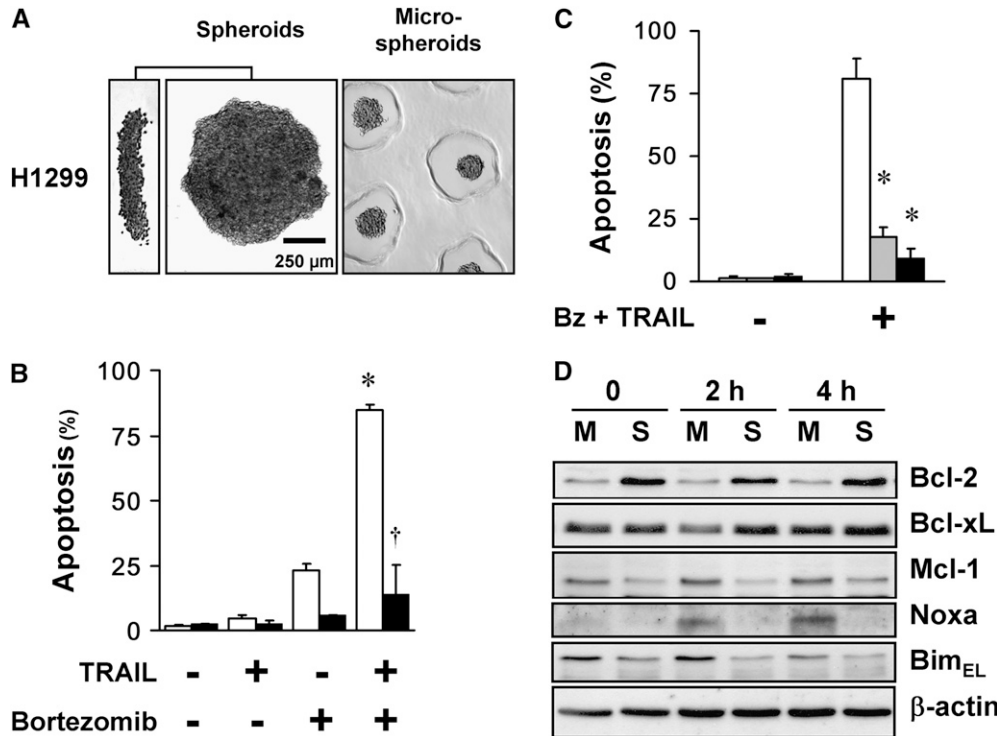


Figure 6. H1299 cells form multicellular spheroids, acquire apoptotic resistance, and demonstrate an altered balance of Bcl-2 family proteins. (A) Spheroids and microspheroids formed from H1299 cells have short diffusion distances. H1299 spheroids generated with 10,000 cells each show a discoid shape and size similar to A549 spheroids, shown from a side view (left panel) and from above (center panel). Microspheroids generated from 250 cells each are spherical, with a diameter of 75–100 μm (representative images shown). (B) H1299 cells in monolayer undergo synergistic apoptosis to the combination of bortezomib plus TRAIL, whereas spheroids exhibit resistance. Bortezomib (100 nM) plus TRAIL (1 ng/ml) for 24 hours induced synergistic apoptosis in H1299 cells grown as monolayers (open bars), the spheroids (solid bars) were resistant to this combinatorial treatment (*different from the sum of the responses to TRAIL alone and to bortezomib alone; †different from monolayer; mean \pm SD; $n = 3$; $P < 0.01$). (C) H1299 microspheroids demonstrate apoptotic resistance similar to spheroids. H1299 cells grown as monolayers (open bars), microspheroids (shaded bars), and spheroids (solid bars) were exposed to 100 nM bortezomib (Bz) plus 1 ng/ml TRAIL for 24 hours, and then studied for apoptosis. Microspheroids and spheroids showed similar apoptotic resistance (*different from monolayer; mean \pm SD; $n = 3$; $P < 0.01$). (D) Expression of Bcl-2 increases and Mcl-1 decreases when H1299 cells form spheroids. A panel of anti- and proapoptotic Bcl-2 family proteins were screened by immunoblot in H1299 monolayers (M) and spheroids (S), before and after treatment with 100 nM bortezomib plus 1 ng/ml TRAIL for 2 and 4 hours. Bcl-2 was up-regulated after H1299 spheroids formed spheroids, whereas Mcl-1 was down-regulated. At 4 hours after treatment, there was a significant up-regulation of Noxa in monolayers, but not in spheroids.

mean \pm SD; $n = 3$; $P < 0.01$). (C) H1299 microspheroids demonstrate apoptotic resistance similar to spheroids. H1299 cells grown as monolayers (open bars), microspheroids (shaded bars), and spheroids (solid bars) were exposed to 100 nM bortezomib (Bz) plus 1 ng/ml TRAIL for 24 hours, and then studied for apoptosis. Microspheroids and spheroids showed similar apoptotic resistance (*different from monolayer; mean \pm SD; $n = 3$; $P < 0.01$). (D) Expression of Bcl-2 increases and Mcl-1 decreases when H1299 cells form spheroids. A panel of anti- and proapoptotic Bcl-2 family proteins were screened by immunoblot in H1299 monolayers (M) and spheroids (S), before and after treatment with 100 nM bortezomib plus 1 ng/ml TRAIL for 2 and 4 hours. Bcl-2 was up-regulated after H1299 spheroids formed spheroids, whereas Mcl-1 was down-regulated. At 4 hours after treatment, there was a significant up-regulation of Noxa in monolayers, but not in spheroids.

Proteasome inhibition has attracted growing interest in the last decade as a cancer-targeting strategy, and the efficacy of proteasome inhibitors, such as bortezomib and the more recent molecules, carfilzomib and NPI-0052, has been widely validated in several hematological malignancies (35). In preclinical studies in NSCLC, bortezomib has been very effective, either used alone or combined with other agents (36–38). Despite the encouraging *in vitro* studies, bortezomib has had disappointing results in clinical trials of patients with NSCLC (17, 18). The greater effectiveness in hematologic malignancies than in most solid tumors suggests that apoptotic resistance to bortezomib may derive from a 3D setting.

In this study, many possible mechanisms for apoptotic resistance to the combinatorial apoptotic strategy in multicellular spheroids were considered and excluded. Limited diffusion of treatments has been suspected as a possible explanation for the reduced efficacy of treatments in solid tumors and 3D spheroids (39). However, in our study, bortezomib inhibited the proteasome activity of monolayers and spheroids to similar levels (see Figure 2A), and TRAIL induced Bid cleavage at similar levels in monolayers and spheroids (see Figure 2B), showing that these two agents were active in the NSCLC spheroids. Apoptotic cells were evenly distributed throughout the spheroid, suggesting adequate diffusion of reagents (see Figure 2D). Inhibition of NF- κ B survival signaling has been considered to represent a major mechanism by which proteasome inhibitors induce apoptosis in tumors (4, 5); however, NF- κ B was not found to be important in our system. For one reason, NF- κ B was not stimulated by TRAIL in our A549 stable reporter cells under the conditions of these experiments, and thus would not have been expected to play a role in survival, unlike in other studies in which TRAIL was

found to induce NF- κ B signaling in H460 lung cancer cells (10) or in A549 cells (40). For another reason, even when activated by TNF, NF- κ B was equally stimulated in monolayers and spheroids, and equally inhibited by bortezomib, indicating that NF- κ B signaling would not account for the differing apoptotic responses between monolayers and spheroids. Akt/mTOR signaling did not mediate apoptotic resistance in A549 spheroids, unlike the situation found in mesothelioma spheroids (21). Finally, FLIP_s up-regulation in spheroids was not found to contribute to this acquired resistance, either by diminishing TRAIL signals proximally or by altering apoptotic resistance generally.

Instead, we found a role for the antiapoptotic Bcl-2 family proteins in spheroid survival and apoptotic resistance. Spheroids exhibited a difference in expression of Bcl-2 family proteins compared with that in monolayers, a difference that was generally maintained after exposure to bortezomib. In monolayers, according to previously published reports and also in our study, bortezomib is known to decrease the expression of antiapoptotic Bcl-2 family proteins, such as Bcl-2, and increase the expression of proapoptotic BH3-only proteins, including Bim and Noxa (6). These proapoptotic changes may be countered by the up-regulation of the antiapoptotic molecule, Mcl-1 (37, 41), a molecule that may account for resistance to bortezomib (6). Although this pattern and the potential role of Mcl-1 in resistance have been well described, the effect of spheroid formation on these proteins and the actions of bortezomib on spheroids has not been addressed previously. We found that spheroid formation of A549 and H1299 cells led to an increase in Bcl-2 and a decrease in Mcl-1 compared with monolayers. After bortezomib, this differential pattern was retained, with Bcl-2 higher in spheroids and Mcl-1 lower in spheroids than in monolayers; in addition, in the

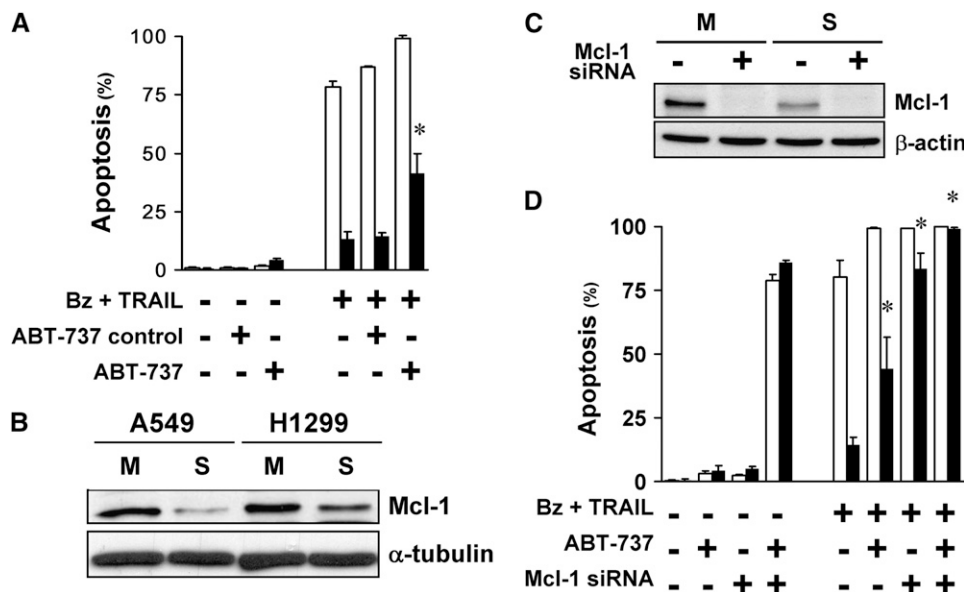


Figure 7. Bcl-2 family proteins contribute to the multicellular resistance of H1299 spheroids. (A) ABT-737 alone did not eliminate the multicellular resistance of spheroids. At baseline, the Bcl-2 family inhibitor, ABT-737, alone (10 μ M) had no effect in H1299 monolayers (*open bars*) and spheroids (*solid bars*). After exposure to bortezomib plus TRAIL, 10 μ M ABT-737 induced an increase in apoptosis of spheroids, but did not eliminate the multicellular resistance. The negative control enantiomer of ABT had no effect (*different from negative control for ABT; mean \pm SD; $n = 3$; $P < 0.01$). (B) H1299 spheroids have higher expression level of Mcl-1 than A549 spheroids. By immunoblot, Mcl-1 was down-regulated in spheroids (S) compared with monolayers (M) in both A549 and H1299 cells. However, H1299 spheroids retained higher expression levels of Mcl-1 than A549 spheroids. (C)

Mcl-1 small interfering RNA (siRNA) depletes the expression of Mcl-1 in H1299 monolayers and spheroids. Mcl-1 was depleted by siRNA, as measured at 48 hours after transfection, the time when apoptotic agents were added. (D) Depletion of Mcl-1 largely removes multicellular resistance in H1299 spheroids. Depletion of Mcl-1 by itself did not induce apoptosis in H1299 monolayers (*open bars*) and spheroids (*solid bars*), but significantly removed the multicellular resistance of H1299 spheroids to 100 nM bortezomib (Bz) plus 1 ng/ml TRAIL treatment for 24 hours. ABT-737 (10 μ M) exposure plus Mcl-1 depletion induced death of monolayers and spheroids, and removed all multicellular resistance to bortezomib plus TRAIL (*different from spheroids treated with bortezomib plus TRAIL; mean \pm SD; $n = 3$; $P < 0.01$).

spheroids, Noxa up-regulation was absent. In observing these changes, we considered that the shift in relative expression of Bcl-2 family members in the spheroids may have altered the relative roles of these antiapoptotic proteins.

Indeed, in A549 cells, blockade with ABT-737, a small molecule inhibitor of Bcl-2, Bcl-xL, and Bcl-w, but not of Mcl-1, revealed that these Bcl-2 proteins had assumed a role in survival not evident in the monolayers. In spheroids, ABT-737 reduced the multicellular resistance to bortezomib plus TRAIL, indicating that these Bcl-2 proteins suppressed the apoptosis induced by this combinatorial therapy. In addition, even in spheroids at baseline, ABT-737 by itself induced apoptosis, indicating that the spheroids had acquired a dependence or an addiction to this apoptotic block for survival (42). Bcl-2 antiapoptotic proteins are thought to sequester BH3-only proapoptotic proteins, thereby preventing them from interacting with Bax and Bak, the proapoptotic molecules necessary for inducing apoptosis (43). The apoptotic response to blockade of the Bcl-2 family indicates that BH3-only molecules, such as Bim, are active, and that the cell is primed to undergo apoptosis if the antiapoptotic brakes are removed (44). The BH3-only molecule Noxa was apparently not required for induction of apoptosis in spheroids by ABT-737, indicating that there were enough other proapoptotic BH3-only molecules, such as Bim, to mediate apoptosis after the removal of the antiapoptotic Bcl-2 block. Thus, we propose that the altered expression of Bcl-2 family proteins in A549 spheroids led to a greater reliance on Bcl-2, as revealed by the response to ABT-737. The reduction of Mcl-1 in the spheroids may have contributed to the shift to Bcl-2; indeed, the addiction to Bcl-2 and the sensitivity to ABT-737 has been shown to become apparent when Mcl-1 is absent or neutralized (45).

Several of these findings were confirmed in H1299 cells, although the relative importance of Mcl-1 exceeded that of Bcl-2. In the treated spheroids, Mcl-1, even though its expression decreased in spheroids, was still sufficient to support multicellular apoptotic resistance to bortezomib plus TRAIL. Blockade

of Bcl-2/Bcl-xL/Bcl-w by ABT had a partial effect, whereas blockade of Mcl-1 nearly completely removed apoptotic resistance. In untreated spheroids, survival was maintained when either Mcl-1 or Bcl-2 alone was blocked, but blockade of both was deadly, suggesting that the cells were primed for death and restrained by either one of these antiapoptotic proteins.

The causes for the changes in expression of Bcl-2 family proteins were not investigated in this study. Bcl-2 can be up-regulated by an elevated NF- κ B (46); however, we did not find increased activity of NF- κ B in spheroids. It is more likely that the up-regulation of Bcl-2 in the 3D spheroids is due to the increased cell adhesion of multicellular spheroids, because Bcl-2 up-regulation has been associated with the engagement of integrins α 5 β 1 (47) or α v β 3 (48). Mcl-1 is known to be tightly regulated by multiple pathways and at multiple levels (49), but, to our knowledge, down-regulation with the transition to 3D has not been reported. Because cells alter their shape, function, and metabolism with aggregation into spheroids, many factors may be involved in the changes in the altered protein expression that we observed.

We have concentrated on the antiapoptotic defenses used by the cancer cell lines in 3D spheroids. Of course, finding an active role for antiapoptotic proteins, such as Bcl-2 or Mcl-1, in maintaining multicellular resistance does not exclude a role for a lack of proapoptotic proteins, such as Noxa, which showed no up-regulation in spheroids after bortezomib. Nonetheless, despite the lack of Noxa, reduction of the antiapoptotic defenses allowed apoptosis, presumably because other proapoptotic BH3-only molecules were active and able to replace the proapoptotic function of Noxa. Inhibition of antiapoptotic molecules is also likely to be a more feasible therapeutic strategy than restoration of proapoptotic molecules. The specific contribution of Bcl-2 family antiapoptotic proteins may differ in different cell lines or in different tumors, but we suggest that antiapoptotic Bcl-2 family proteins may represent a final common denominator of multicellular resistance and one that is amenable to therapeutic manipulation.

In conclusion, this study demonstrates that lung cancer spheroids acquire multicellular resistance to bortezomib plus TRAIL and that Bcl-2 family proteins contribute to this acquired resistance. The multicellular resistance found in 3D spheroids may model the therapeutic resistance found in solid tumors. The antiapoptotic Bcl-2 family proteins might be attractive targets to increase the clinical efficacy of bortezomib against lung cancer.

Conflict of Interest Statement: None of the authors has a financial relationship with a commercial entity that has an interest in the subject of this manuscript.

References

- Bremer E, van Dam G, Kroesen BJ, de Leij L, Helfrich W. Targeted induction of apoptosis for cancer therapy: current progress and prospects. *Trends Mol Med* 2006;12:382–393.
- Broaddus VC, Dansen TB, Abayasiriwardana KS, Wilson SM, Finch AJ, Swigart LB, Hunt AE, Evan GI. Bid mediates apoptotic synergy between tumor necrosis factor-related apoptosis-inducing ligand (TRAIL) and DNA damage. *J Biol Chem* 2005;280:12486–12493.
- Lowe SW, Cepero E, Evan GI. Intrinsic tumour suppression. *Nature* 2004;432:307–315.
- Milligan SA, Nopajaroonsri C. Inhibition of NF-kappa B with proteasome inhibitors enhances apoptosis in human lung adenocarcinoma cells *in vitro*. *Anticancer Res* 2001;21:39–44.
- An J, Sun Y, Fisher M, Rettig MB. Maximal apoptosis of renal cell carcinoma by the proteasome inhibitor bortezomib is nuclear factor-kappaB dependent. *Mol Cancer Ther* 2004;3:727–736.
- Fennell DA, Chacko A, Mutti L. BCL-2 family regulation by the 20S proteasome inhibitor bortezomib. *Oncogene* 2008;27:1189–1197.
- Mortenson MM, Schlieman MG, Virudachalam S, Lara PN, Gandara DG, Davies AM, Bold RJ. Reduction in BCL-2 levels by 26S proteasome inhibition with bortezomib is associated with induction of apoptosis in small cell lung cancer. *Lung Cancer* 2005;49:163–170.
- Fahy BN, Schlieman MG, Mortenson MM, Virudachalam S, Bold RJ. Targeting BCL-2 overexpression in various human malignancies through NF-kappaB inhibition by the proteasome inhibitor bortezomib. *Cancer Chemother Pharmacol* 2005;56:46–54.
- Sayers TJ, Murphy WJ. Combining proteasome inhibition with TNF-related apoptosis-inducing ligand (Apo2L/TRAIL) for cancer therapy. *Cancer Immunol Immunother* 2006;55:76–84.
- Voortman J, Resende TP, Abou El Hassan MA, Giaccone G, Krut FA. TRAIL therapy in non-small cell lung cancer cells: sensitization to death receptor-mediated apoptosis by proteasome inhibitor bortezomib. *Mol Cancer Ther* 2007;6:2103–2112.
- Liu X, Yue P, Chen S, Hu L, Lonial S, Khuri FR, Sun SY. The proteasome inhibitor PS-341 (bortezomib) up-regulates DR5 expression leading to induction of apoptosis and enhancement of TRAIL-induced apoptosis despite up-regulation of c-FLIP and survivin expression in human NSCLC cells. *Cancer Res* 2007;67:4981–4988.
- Coticello C, Adamo L, Giuffrida R, Vicari L, Zeuner A, Eramo A, Anastasi G, Memeo L, Giuffrida D, Iannolo G, et al. Proteasome inhibitors synergize with TRAIL to induce anaplastic thyroid carcinoma cell death. *J Clin Endocrinol Metab* 2007;92:1938–1942.
- Johnson TR, Stone K, Nikrad M, Yeh T, Zong WX, Thompson CB, Nesterov A, Kraft AS. The proteasome inhibitor PS-341 overcomes TRAIL resistance in Bax and caspase 9-negative or Bcl-xL overexpressing cells. *Oncogene* 2003;22:4953–4963.
- Kyritsis AP, Tachmazoglou F, Rao JS, Puduvali VK. Bortezomib sensitizes human astrocytoma cells to tumor necrosis factor related apoptosis-inducing ligand induced apoptosis. *Clin Cancer Res* 2007;13:6540–6541. (author reply 6541–6542).
- Richardson PG, Sonneveld P, Schuster M, Irwin D, Stadtmauer E, Facon T, Harousseau JL, Ben-Yehuda D, Lonial S, Goldschmidt H, et al. Extended follow-up of a phase 3 trial in relapsed multiple myeloma: final time-to-event results of the APEX trial. *Blood* 2007;110:3557–3560.
- Kropff M, Bisping G, Schuck E, Liebisch P, Lang N, Henrich M, Dechow T, Kroger N, Salwender H, Metzner B, et al. Bortezomib in combination with intermediate-dose dexamethasone and continuous low-dose oral cyclophosphamide for relapsed multiple myeloma. *Br J Haematol* 2007;138:330–337.
- Fanucchi MP, Fossella FV, Belt R, Natale R, Fidas P, Carbone DP, Govindan R, Raez LE, Robert F, Ribeiro M, et al. Randomized phase II study of bortezomib alone and bortezomib in combination with docetaxel in previously treated advanced non-small-cell lung cancer. *J Clin Oncol* 2006;24:5025–5033.
- Lara PN Jr, Koczywas M, Quinn DI, Lenz HJ, Davies AM, Lau DH, Gumerlock PH, Longmate J, Doroshow JH, Schenkein D, et al. Bortezomib plus docetaxel in advanced non-small cell lung cancer and other solid tumors: a phase I California Cancer Consortium trial. *J Thorac Oncol* 2006;1:126–134.
- Pampaloni F, Reynaud EG, Stelzer EH. The third dimension bridges the gap between cell culture and live tissue. *Nat Rev Mol Cell Biol* 2007;8:839–845.
- Smalley KS, Lioni M, Herlyn M. Life isn't flat: taking cancer biology to the next dimension. *In Vitro Cell Dev Biol Anim* 2006;42:242–247.
- Barbone D, Yang TM, Morgan JR, Gaudino G, Broaddus VC. Mammalian target of rapamycin contributes to the acquired apoptotic resistance of human mesothelioma multicellular spheroids. *J Biol Chem* 2008;283:13021–13030.
- Wilson SM, Barbone D, Yang TM, Jablons DM, Bueno R, Sugarbaker DJ, Nishimura SL, Gordon GJ, Broaddus VC. mTOR mediates survival signals in malignant mesothelioma grown as tumor fragment spheroids. *Am J Respir Cell Mol Biol* 2008;39:576–583.
- Napolitano AP, Chai P, Dean DM, Morgan JR. Dynamics of the self-assembly of complex cellular aggregates on micromolded nonadhesive hydrogels. *Tissue Eng* 2007;13:2087–2094.
- Lai C, Jiang X, Li X. Development of luciferase reporter-based cell assays. *Assay Drug Dev Technol* 2006;4:307–315.
- Torres Filho IP, Leung M, Yuan F, Intaglietta M, Jain RK. Noninvasive measurement of microvascular and interstitial oxygen profiles in a human tumor in SCID mice. *Proc Natl Acad Sci USA* 1994;91:2081–2085.
- Wang X, Wang Y, Zhang J, Kim HP, Ryter SW, Choi AM. FLIP protects against hypoxia/reoxygenation-induced endothelial cell apoptosis by inhibiting Bax activation. *Mol Cell Biol* 2005;25:4742–4751.
- Wilson TR, McLaughlin KM, McEwan M, Sakai H, Rogers KM, Redmond KM, Johnston PG, Longley DB. c-FLIP: a key regulator of colorectal cancer cell death. *Cancer Res* 2007;67:5754–5762.
- Sharp DA, Lawrence DA, Ashkenazi A. Selective knockdown of the long variant of cellular FLICE inhibitory protein augments death receptor-mediated caspase-8 activation and apoptosis. *J Biol Chem* 2005;280:19401–19409.
- Oltersdorf T, Elmore SW, Shoemaker AR, Armstrong RC, Fesik SW, Rosenberg SH. An inhibitor of Bcl-2 family proteins induces regression of solid tumours. *Nature* 2005;435:677–681.
- Tahir SK, Yang X, Anderson MG, Morgan-Lappe SE, Sarthy AV, Chen J, Warner RB, Ng SC, Fesik SW, Elmore SW, et al. Influence of Bcl-2 family members on the cellular response of small-cell lung cancer cell lines to ABT-737. *Cancer Res* 2007;67:1176–1183.
- Hanahan D, Weinberg RA. The hallmarks of cancer. *Cell* 2000;100:57–70.
- Shivapurkar N, Reddy J, Chaudhary PM, Gazdar AF. Apoptosis and lung cancer: a review. *J Cell Biochem* 2003;88:885–898.
- Pommier Y, Sordet O, Antony S, Hayward RL, Kohn KW. Apoptosis defects and chemotherapy resistance: molecular interaction maps and networks. *Oncogene* 2004;23:2934–2949.
- Olive PL, Durand RE. Drug and radiation resistance in spheroids: cell contact and kinetics. *Cancer Metastasis Rev* 1994;13:121–138.
- Orlowski RZ, Kuhn DJ. Proteasome inhibitors in cancer therapy: lessons from the first decade. *Clin Cancer Res* 2008;14:1649–1657.
- Voortman J, Checinska A, Giaccone G, Rodriguez JA, Krut FA. Bortezomib, but not cisplatin, induces mitochondria-dependent apoptosis accompanied by up-regulation of noxa in the non-small cell lung cancer cell line NCI-H460. *Mol Cancer Ther* 2007;6:1046–1053.
- Jung CS, Zhou Z, Khuri FR, Sun SY. Assessment of apoptosis-inducing effects of docetaxel combined with the proteasome inhibitor PS-341 in human lung cancer cells. *Cancer Biol Ther* 2007;6:749–754.
- Schenkein DP. Preclinical data with bortezomib in lung cancer. *Clin Lung Cancer* 2005;7:S49–S55.
- Tannock IF, Lee CM, Tunggal JK, Cowan DS, Egorin MJ. Limited penetration of anticancer drugs through tumor tissue: a potential cause of resistance of solid tumors to chemotherapy. *Clin Cancer Res* 2002;8:878–884.
- Lee KY, Park JS, Jee YK, Rosen GD. Triptolide sensitizes lung cancer cells to TNF-related apoptosis-inducing ligand (TRAIL)-induced apoptosis by inhibition of NF-kappaB activation. *Exp Mol Med* 2002;34:462–468.
- Voortman J, Checinska A, Giaccone G. The proteasomal and apoptotic phenotype determine bortezomib sensitivity of non-small cell lung cancer cells. *Mol Cancer* 2007;6:73–79.
- Letai AG. Diagnosing and exploiting cancer's addiction to blocks in apoptosis. *Nat Rev Cancer* 2008;8:121–132.

43. Letai AG, Bassik MC, Walensky LD, Sorcinelli MD, Weiler S, Korsmeyer SJ. Distinct BH3 domains either sensitize or activate mitochondrial apoptosis, serving as prototype cancer therapeutics. *Cancer Cell* 2002;2:183–192.
44. Deng J, Carlson N, Takeyama K, Dal Cin P, Shipp M, Letai AG. BH3 profiling identifies three distinct classes of apoptotic blocks to predict response to ABT-737 and conventional chemotherapeutic agents. *Cancer Cell* 2007;12:171–185.
45. van Delft MF, Wei AH, Mason KD, Vanderberg CJ, Chen L, Czabotar PE, Willis SN, Scott CL, Day CL, Cory S, *et al.* The BH3 mimetic ABT-737 targets selective Bcl-2 proteins and efficiently induces apoptosis via Bak/Bax if Mcl-1 is neutralized. *Cancer Cell* 2006;10:389–399.
46. Konishi T, Sasaki S, Watanabe T, Kitayama J, Nagawa H. Overexpression of hRFI inhibits 5-fluorouracil-induced apoptosis in colorectal cancer cells via activation of NF-kappaB and upregulation of BCL-2 and BCL-XL. *Oncogene* 2006;25:3160–3169.
47. Lee BH, Ruoslahti E. Alpha5beta1 integrin stimulates Bcl-2 expression and cell survival through Akt, focal adhesion kinase, and Ca²⁺/calmodulin-dependent protein kinase IV. *J Cell Biochem* 2005;95:1214–1223.
48. Matter ML, Ruoslahti E. A signaling pathway from the alpha5beta1 and alpha(v)beta3 integrins that elevates Bcl-2 transcription. *J Biol Chem* 2001;276:27757–27763.
49. Warr MR, Shore GC. Unique biology of Mcl-1: therapeutic opportunities in cancer. *Curr Mol Med* 2008;8:138–147.